

Side-by-side silicon carbide–silica biaxial nanowires: Synthesis, structure, and mechanical properties

Z. L. Wang,^{a)} Z. R. Dai, R. P. Gao,^{b)} and Z. G. Bai

School of Materials Science and Engineering, Georgia Institute of Technology, Atlanta, Georgia 30332-0245

J. L. Gole^{c)}

School of Physics, Georgia Institute of Technology, Atlanta, Georgia 30332-0400

(Received 10 July 2000; accepted for publication 19 September 2000)

Elevated-temperature synthesis has been used to generate side-by-side biaxially structured silicon carbide–silica nanowires. The axial growth direction approaches [311] for nanowires with a high density of microtwins and is [211] for defect-free nanowires. The structure of these nanowires, their cross-sectional shape, and their structural transformation between a biaxial and coaxial configuration have been studied by transmission electron microscopy. The Young's modulus of the biaxially structured nanowires was measured to be 50–70 GPa depending on the size of the nanowire. © 2000 American Institute of Physics. [S0003-6951(00)02347-0]

One-dimensional quantum wires are of fundamental importance to the study of size-dependent chemical and physical phenomena. The properties of nanowires may sensitively depend on their geometrical shape/configurations, which can include tubular structures (multi/single-walled carbon nanotubes), solid cylindrical nanowires,^{1–3} or coaxial constructions.⁴ Devices made using nanowire heterojunctions can be critical for nanoelectronics.^{5,6} Silicon carbide is a wide band gap semiconducting material used for high-temperature, high-frequency, and high-power applications. The growth of β -SiC whiskers can be achieved using a variety of well-established techniques. Recently, Lieber,¹ Lee,² Yu,³ and co-workers have extrapolated on the ideas entailed in the vapor–liquid–solid technique to develop the laser ablation of metal containing silicon targets as a means of obtaining bulk quantities of silicon nanowires. Here, we report the synthesis of bulk quantities of biaxially structured silicon carbide–silica nanowires, composed of side-by-side sub-nanowires. We have applied the techniques of high-temperature synthesis to modify and generalize the approach of Lee *et al.*² to synthesize dislocation-free Si nanowires, as reported in detail elsewhere.⁷ In the current letter, amorphous SiO is brought into intimate contact with carbon/graphite in an appropriate mix at elevated temperatures for an extended time period. To produce the biaxial silicon carbide–silica nanowire configurations, the system was operated at temperatures close to 1500 °C for 12 h.

Figure 1(a) depicts a low-magnification transmission electron microscopy (TEM) image of the nanowires dispersed on a carbon film. The nanowires are uniform with diameter 50–80 nm, and a length which can be as long as 100 μ m. The as-synthesized materials are grouped into three basic nanowire structures: pure SiO_x nanowires, coaxially SiO_x sheathed β -SiC nanowires [Fig. 1(b)] (~50% of material), and biaxial β -SiC–SiO_x nanowires [Fig. 1(c)] (~30% of material). The coaxial SiC–SiO_x nanowires have a {111}

growth direction with a high density of twins and stacking faults perpendicular to this growth direction. From the cross-sectional TEM images of the as-synthesized nanowires, the geometrical shapes of the coaxial SiC–SiO_x [Fig. 1(d)] and the biaxial SiC–SiO_x nanowires [Figs. 1(e) and 1(f)] are unambiguously revealed. The SiC nanowires have faceted shapes, and one type of the facet is {111}. The objective of this letter is to study the growth mechanism and the mechanical properties of the biaxial nanowires.

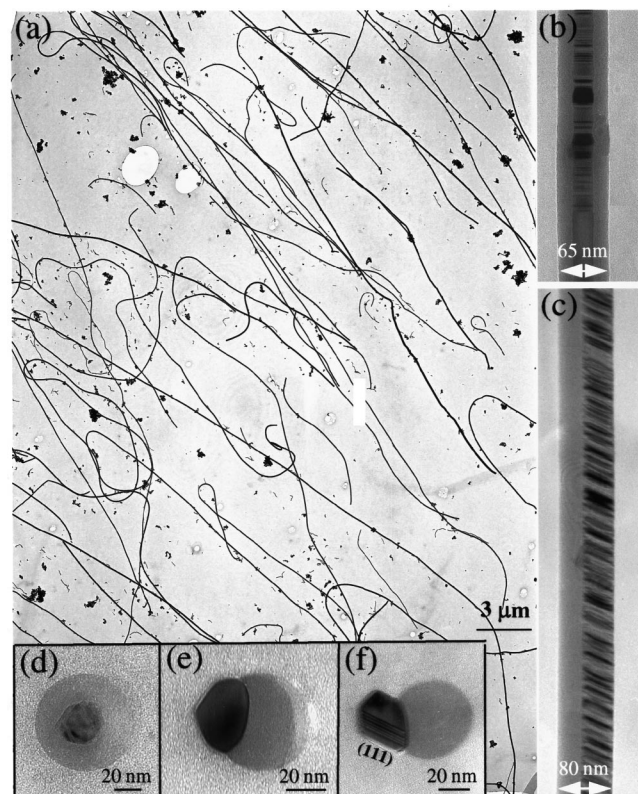


FIG. 1. (a) Low-magnification TEM image of the as-synthesized nanowires supported by a carbon film, showing their ultralong length and uniformity in diameter. Side views of a (b) coaxially and (c) biaxially structured SiC–SiO_x nanowire. (d), (e), and (f) Cross-sectional TEM images of coaxially structured SiC–SiO_x and biaxially structured SiC–SiO_x nanowires, respectively.

^{a)}Author to whom all correspondence should be addressed; electronic mail: zhong.wang@mse.gatech.edu

^{b)}Also at: University of Science and Technology Beijing, Beijing, China.

^{c)}Electronic mail: james.gole@physics.gatech.edu

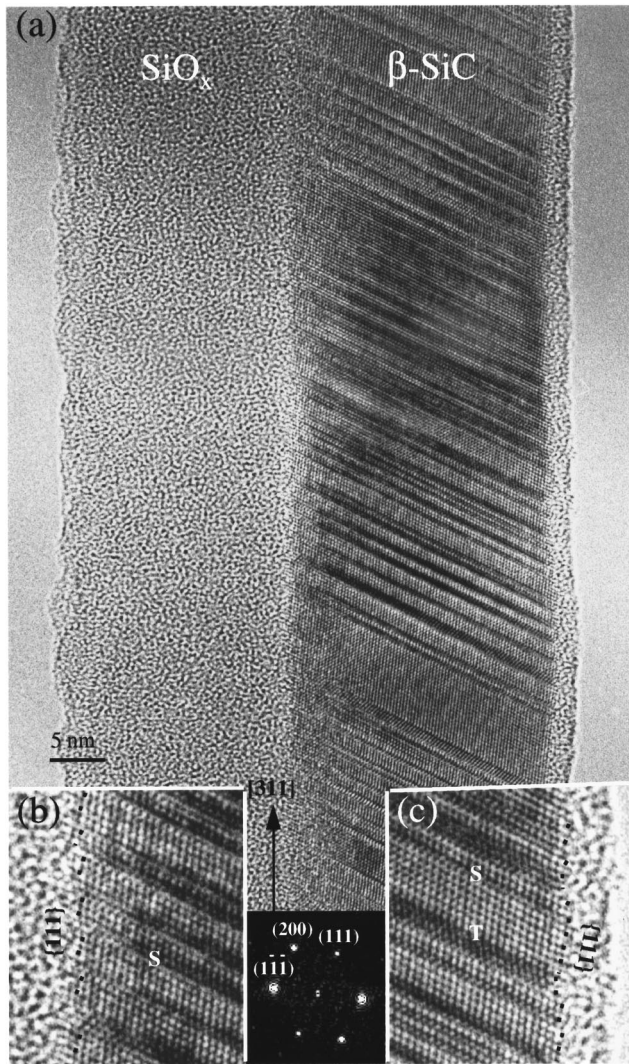


FIG. 2. High-resolution TEM image of a biaxially structured β -SiC-SiO_x nanowire, showing the crystallographic and defect structures of the nanowire. The electron beam is along $[01\bar{1}]$, perpendicular to the nanowire. A Fourier transform of the image from a defect-free area, given at the bottom, shows that the growth direction of the nanowire is $[311]$. (b) and (c) Enlargements of the areas between the interfaces of SiO_x-SiC at the contact area and near the surface of SiC-SiO_x, respectively, showing the $\{111\}$ faceted nanoareas at the interface. *S* and *T* stand for stacking fault and twin, respectively.

The biaxial SiC-SiO_x nanowires consist of two side-by-side subnanowires of silica and β -SiC [Fig. 2(a)], which can be simply referred to as a composite nanowire. If we image from the $[01\bar{1}]$ direction perpendicular to the nanowire, the overlap between the amorphous SiO_x side and the β -SiC is only ~ 4 nm. There is also a thin layer of silica passivated on the surface of the β -SiC. The β -SiC side has a high density of stacking faults and a few twins (so-called microtwins). This can be seen more clearly in an enlargement of a local region [Fig. 2(b)], where the outermost surface of the β -SiC is composed of nanosize $\{111\}$ facets. At the interface between SiC and SiO_x, small segments of $\{111\}$ faces are also identified [Fig. 2(c)]. The presence of a high density of planar defects results in a $[311]$ axial direction for the biaxial nanowires, in contrast to $[111]$ for the coaxial nanowires.⁴ Biaxial nanowires with a much lower density of stacking faults and a $[211]$ growth direction have also been observed occasionally.

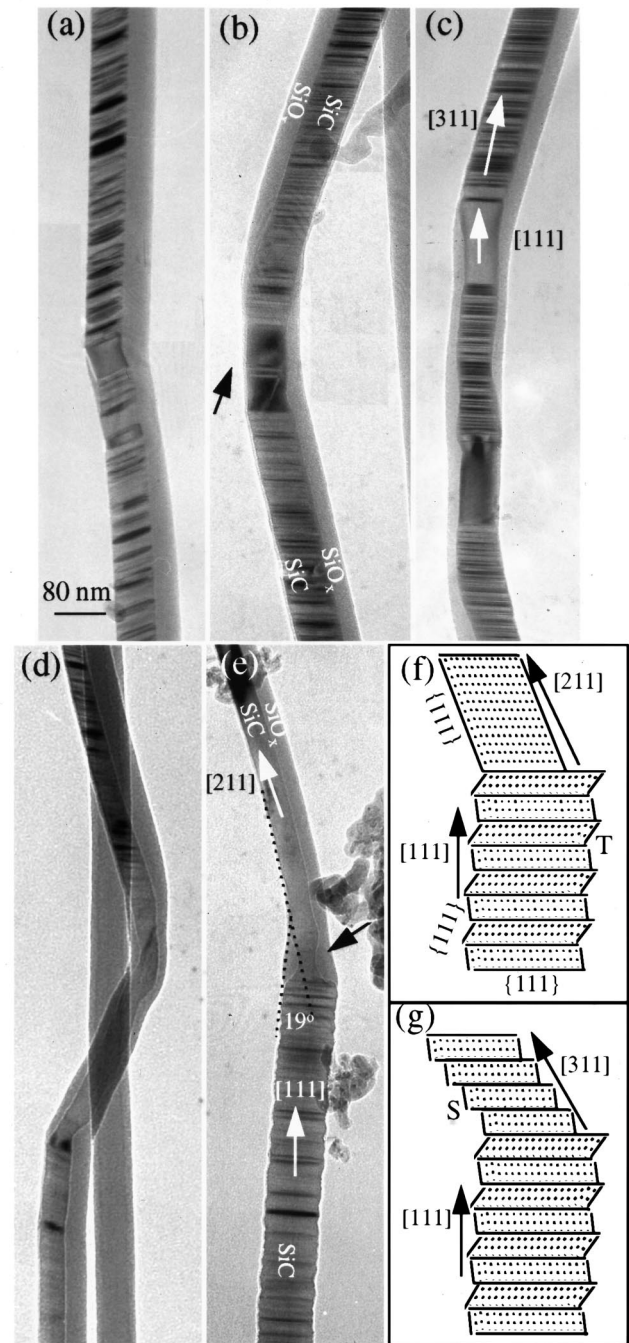


FIG. 3. (a)-(d) TEM images from the SiC-SiO_x biaxially structured nanowires, displaying structural evolutions and interface junctions in the nanowires. Bending appears wherever a defect free segment is created due to a change in growth direction from $[311]$ or $[211]$ to $[111]$. The electron beam is near $[01\bar{1}]$. (e) Structural transformation from a coaxial to biaxial nanowire, where a neck-shape junction is formed at the interfacial region. (f), (g) Models for the structural transformation from a coaxial to a biaxial nanowire growing along the $[211]$ and $[311]$ directions.

Shown in Fig. 3 are a group of TEM images that indicate the structural transformation in the SiC-SiO_x nanowire systems. The segment containing a high density of planar defects grows straight along the axis, while the presence of a defect free region results in bending [Figs. 3(a)-3(c)] and sharp turns [Fig. 3(d)] along the nanowires. This is the result of switching the growth direction from $[311]$ or $[211]$ for the biaxial structure to $[111]$ for the coaxial structure, while a common (111) plane is preserved. It is important to note that the SiC and SiO_x sides also switch across a bending area

TABLE I. Measured Young's modulus of coaxial cable structured SiC-SiO_x nanowires (SiC is the core, and silica is the sheath). ($\rho_{\text{silica}}=2.2 \times 10^3 \text{ kg/m}^3$; $\rho_{\text{SiC}}=3.2 \times 10^3 \text{ kg/m}^3$).

D_s (nm) (± 2 nm)	D_c (nm) (± 1 nm)	L (μm) ($\pm 0.2 \mu\text{m}$)	f_0 (MHz)	E_{eff} (GPa) Expt	E_{eff} (GPa) Theor
51	12.5	6.8	0.693	46 \pm 9.0	73
74	26	7.3	0.953	56 \pm 9.2	78
83	33	7.2	1.044	52 \pm 8.2	82
132	48	13.5	0.588	78 \pm 7.0	79
190	105	19.0	0.419	81 \pm 5.1	109

[Figs. 3(b)–3(d)] while the orientation of the planar defects does not change significantly. This indicates an exchange in position of the two sides rather than a twisting along the growth direction.

Figure 3(c) shows a case in which a short segment of coaxial nanowire (along [111]) links two biaxially structured nanowires as the side-by-side SiC and SiO_x subnanowires are exchanged. This is the case of an interface junction between biaxial and coaxial nanowires in the same nanomaterial. Figure 3(e) displays a case of structural transformation from coaxial growth to biaxial growth. The transition region is a thin neck and the twin results in the bending of the nanowire.

The unique structure of the nanowire is likely determined by growth kinetics. To propose a mechanism for the structural transformation from a coaxial to a biaxial nanowire, we introduce a structure block, based on the high-resolution TEM image shown in Fig. 2, which is enclosed by {111} facets as viewed along [01 $\bar{1}$]. Although each block is a defect-free crystal slab of SiC, stacking faults and twins are introduced in stacking the blocks into a wire structure [Fig. 3(f)]. If the density of the twins is dominant, the nanowire grows along [111]. The growth direction switches to [211] if a larger defect-free block is stacked onto the (111) plane [Fig. 3(f)]. Alternatively, if the density of stacking faults is high so that there is a constant translation between the adjacent blocks toward one direction, the nanowire is likely to grow along [311] or an alternate direction depending on the relative shift between the blocks [Fig. 3(g)]. The atomic-scale kinks and ledges created by the formation of the [311] nanowire may increase the surface energy. Thus, to minimize the surface energy, a silica subnanowire is likely to form adjacent to the SiC subnanowire on its rough surface. This process may operate simultaneously with kinetics to determine the development of silica passivation.

The synthesized nanowires could be potentially useful for high-strength composites, in which mechanical properties are critical. We have recently developed an approach that uses *in situ* TEM^{8,9} as an effective tool for measuring the properties of individual carbon nanotubes. This technique is based on electric field induced dynamic resonance phenomena, is nanowire selective, and can easily be applied to any wire-structured nanomaterials. Here, one end of the nanowire is fixed onto a gold ball using conductive glue, and an oscillating voltage is applied across the ball and its counter electrode. Mechanical resonance occurs when the applied frequency matches the natural resonance frequency, however, care must be exercised in identifying the fundamental resonance frequency.⁸

TABLE II. Measured Young's modulus of biaxially structured SiC-SiO_x nanowires. D_{wire} and D_{SiC} are the widths across the entire nanowire and across the SiC subnanowire, respectively.

D_{wire} (nm) (± 2 nm)	D_{SiC} (nm) (± 1 nm)	L (μm) ($\pm 0.2 \mu\text{m}$)	f_0 (MHz)	E_{eff} (GPa) Expt
58	24	4.3	1.833	54 \pm 24.1
70	36	7.9	0.629	53 \pm 8.4
83	41	4.3	2.707	61 \pm 13.8
92	47	5.7	1.750	64 \pm 14.3

For a beam with one end hinged and the other free, the resonance frequency is given by¹⁰

$$f_0 = (\beta^2/2\pi)(EI/m)^{1/2}/L^2,$$

where f_0 is the fundamental resonance frequency, $\beta = 1.875$, EI is the flexural rigidity (or bending stiffness), E is the Young's modulus, I is the moment of inertia about a particular axis of the rod, L is the length of the beam, and m is its mass per unit length. For a coaxial cable structured nanowire whose core material density is ρ_c and diameter is D_c and a sheath material density which is ρ_s with outer diameter D_s , the average density of the nanowire is given by $\rho_e = \rho_c(D_c^2/D_s^2) + \rho_s(1 - D_c^2/D_s^2)$. The effective Young's modulus of the composite nanowire, $E_{\text{eff}} = \rho_e[8\pi f_0 L^2/\beta^2 D_s]^2$. The bending modulus for the coaxial cable structured SiC-SiO_x nanowires results in combination from SiC and SiO_x. The bending modulus increases as the diameter of the nanowire increases (Table I), consistent with the theoretically expected values of $E_{\text{eff}} = \alpha E_{\text{SiC}} + (1 - \alpha)E_{\text{silica}}$, where $\alpha = (D_c/D_s)^4$. The data match well to the calculated values for larger diameter nanowires.

From the cross-sectional TEM image of a biaxially structured nanowire displayed in Fig. 1(e), the outermost contour of the cross-section of the nanowire can be approximated to be elliptical. Thus, the effective Young's modulus of the nanowire can be calculated using the formula for a uniform beam with the introduction of an effective moment of inertia and density. The experimentally measured Young's modulus is given in Table II.

The authors are thankful for support from the US NSF Grant No. DMR-9733160 and the NSF of China.

¹A. M. Morales and C. M. Lieber, *Science* **279**, 208 (1998).

²S. T. Lee, N. Wang, Y. F. Zhang, and Y. H. Tang, *Mater. Res. Bull.*, **36** (August 1999).

³D. P. Yu, Z. G. Bai, Y. Ding, Q. L. Hang, H. Z. Zhang, J. J. Wang, Y. H. Zou, W. Qian, G. C. Xiong, H. T. Zhou, and S. Q. Feng, *Appl. Phys. Lett.* **72**, 3458 (1998).

⁴Y. Zhang, K. Suenaga, C. Colliex, and S. Iijima, *Science* **281**, 973 (1998).

⁵J. Hu, M. Ouyang, P. Yang, and C. M. Lieber, *Nature (London)* **399**, 48 (1999).

⁶Y. Q. Zhu, W. B. Hu, W. K. Hsu, M. Terrones, N. Grobert, J. P. Hare, H. W. Kroto, D. R. M. Walton, and H. Terrones, *J. Mater. Chem.* **9**, 3173 (1999).

⁷J. L. Gole, J. D. Scout, W. L. Rauch, and Z. L. Wang, *Appl. Phys. Lett.* **76**, 2346 (2000).

⁸P. Poncharal, Z. L. Wang, D. Ugarte, and W. A. de Heer, *Science* **283**, 1516 (1999).

⁹Z. L. Wang, P. Poncharal, and W. A. de Heer, *Pure Appl. Chem.* **72**, 209 (2000).

¹⁰L. Meirovich, *Elements of Vibration Analysis* (McGraw-Hill, New York, 1986).